ONE SHOT OPTICAL 3D SURFACE RECONSTRUCTION OF WEAK TEXTURED OBJECTS FOR AN AGRICULTURAL APPLICATION

Martin Laurowski, Thomas Kerstein#, Philipp Klein*,*
Michael Weyrich, Hubert Roth#, Jürgen Wahrburg#*

*University of Siegen, Chair of Automated Manufacturing and Assembly
Paul-Bonatz-Straße 9-11
D-57068 Siegen
Phone: +49 (0) 271/740-2338
E-Mail: laurowski@zess.uni-siegen.de

#University of Siegen, Chair of Automatic Control Engineering
Hoelderlinstr. 3
D-57068 Siegen
Phone: +49 (0) 271/740-2450
E-Mail: kerstein@zess.uni-siegen.de

ABSTRACT

Optical 3D measurement is meaningful in numerous industrial applications. In various cases, the objects to be measured moreover contain only sparse or even no texture. Predestinated examples are agricultural products like peeled potato tubers as well as industrial repetition parts made of plastic or ceramic, such as housing parts or ceramic bottles. These parts are often conveyed in a wobbling way during the automated optical inspection. Thus, conventional 3D shape acquisition methods like laser scanning might fail. In this paper, a novel approach for acquiring 3D shape of weak textured and moving objects is presented. It is primarily intended for automated optical quality assurance in field of agricultural processing industry. To facilitate such measurements, an active stereo vision system with structured light is proposed. The system consists of multiple camera pairs and auxiliary laser pattern generators. The shape acquisition is performed within one shot and is therefore beneficial for rapid inspection tasks. An experimental setup, including hardware and software, has been developed and implemented.

Index Terms – automated inspection, optical, imaging, quality assurance

1. INTRODUCTION

Surface reconstruction and 3D modeling are nowadays standard methods in various applications. Inspection tasks in industrial environment such as agricultural and food industry, reverse engineering, augmented and virtual reality applications, as well as medical applications are typical application fields. In addition, a current demand is contactless inspection, especially for sensitive products and production environments with hygienic requirements. Surface inspection and 3D shape reconstruction can be combined to detect and localize defects on objects automatically for optical inspection tasks in an industrial environment. The inspection results can be used in order to control a subsequent sorting or machining process [1], [2].

2. OBJECTIVES, PROBLEM FORMULATION, REQUIREMENTS

2.1. **Objective**

In this paper, a combination of geometry determination and surface inspection is presented. It allows a quick and robust automatic surface reconstruction of weak textured objects, focused on natural products, such as food products. However it can also be applied to general industrial applications like the inspection of plastic, ceramic or coated objects with curved surfaces. A common criterion of all intended applications is the necessity of the acquisition of a scene in one-shot due to several conditions in the considered application fields.

2.2. **Problem formulation**

Different methods, which could be classified as scanning and non-scanning methods, can be used for the geometry determination. If a defined relative motion between camera and object is performed, an application is suitable for a scanning procedure. In contrast, many applications require simultaneously acquisition of entire objects from multiple perspectives. Multiple, continuously moving objects have to be acquired per second. The continuous movement on a conveyor belt would principally allow the scanning imaging method. However these methods could lead to errors in the registration because the objects might perform additional transversal movements regarding to the main transport direction. This problem is avoided by an acquisition of the entire object with one shot.

Analyzing geometric features of agricultural products, especially if they are peeled is exemplary more difficult because of the weak textured surfaces then determining other industrial products. The presented approach allows for the reconstruction of shapes of surfaces even without any texture. Here "texture" is defined as the characteristic surface features and patterns which can be distinguished by an optical system.

One task in the context of industrial quality control often is the inspection of geometrical accuracy of products. In comparison, the geometry of natural goods is subject to volatility. A certain a priori knowledge of the shape of the object exists, but their exact forms and sizes may vary significantly. Nevertheless, the industrial processing of food is a mass production with extremely large quantities. The time intervals for parts examination are quite short and often below one second.

2.3. **Requirements for a given application**

Different requirements for the inspection task result from the described fields of application. These have to be met with the presented approach. Only a low accuracy is economically viable because of the following machining implemented in the industrial process. Therefore, a depth resolution in the range of +/- 1.5 mm is sufficient for the detection of the surface geometry. The size of the testing objects is in the range of a few centimeters in diameter. A prismatic measurement volume of width 150 mm x length 150 mm x height 100 mm is defined. These dimensions are based on the size of the inspected parts and constrains of the mechanical integration space. The shape of the objects does not need to be completely captured, as long a priori knowledge is available. The geometry of the objects varies in a certain range within the specification. Missing areas of geometry can be reconstructed, based on a statistically model. As a representative typical application we identified the processing of peeled potato tubers.

Up to five objects per second should be processed. This corresponds to a cycle time of about 0.2 s. In addition, a robust mode in rough industrial environments should be possible with the system, which should be developed. Robust mode in this context means that the method works under adverse conditions delivering expected accuracy and high reliability. Changes in the color gradation of the object must not affect the geometry of acquisition. In addition, possible rocking and swinging motions of the conveyor system have to be compensated.

Geometry and surface must be acquired simultaneously, because the objects are not guided. The frame rate of the camera is the limiting factor for the temporal resolution of the image acquisition. The demand for one shot acquisition results from these requirements.

3. STATE OF THE ART

In this investigation, numerous approaches for optical acquisition of object geometry, are investigated in order to find a system fulfilling the requirements of the inspection task. This survey is one part of the research work. A survey on methods for surface and 3D-acquisition reveals a wide variety of automated inspection methods. Within the variety of approaches there are two main groups in techniques of shape reconstruction - direct and indirect methods. A classification is presented in Fig. 1. Further general information on depth estimation systems can be found in [3]. In the following section, an overview of significant methods according to the boundary condition of the inspection task, is given.

3.1. **Time of flight**

This method also abbreviated as PMD (Photonic Mixer Device) uses modulated pulsed infrared light and reconstructs the depth information from the time-of-flight. It is described in [4], [5].

3.2. **Depth from focus**

Depth from Focus recovers the shape of an object from two-dimensional images. A new depth from focus algorithm which improves the recovered shape of weak textured objects is proposed in [6].

3.3. **Triangulation**

Active vision with structured light: The geometry estimation is based on an area scan camera and a line laser module. In order to capture the whole object geometry a relative movement between camera and object is required. A combination of the methods shape from structured light and shape from silhouette is proposed in [8]. Some approaches for geometry acquisition by a laser scanner are described in [9], [10] and [11].

A technique for shape reconstruction in dynamic scenes and on objects with weak textures, which requires only a single-frame image of a structured light grid pattern, is proposed in [12]. A monocular system for depth estimation with an infrared (IR) camera and IR-pattern projector (trade name Kinect) working as light sheet system is offered by [13].

Stereo vision approaches can in general be divided in passive and active.

3.3.1. Passive stereo vision

The 3D information of an object is reconstructed from a stereo camera setup and an unstructured light source. In [14], a two cameras vision model for the 3D shape recognition, is described. An industrial 3D vision system for real-time applications using stereo is presented by [15]. An effective method to accurately reconstruct and measure the 3D curve edges is mentioned by [16]. In [17] a system for simultaneously obtaining data from 2D and 3D images is presented. An approach for monocular stereo with a plenoptic light field camera is described in [18] and [19].

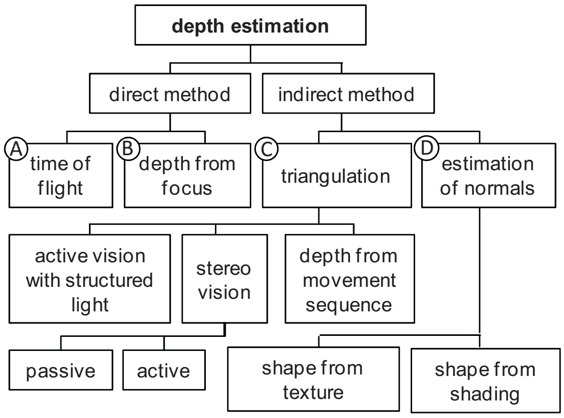

Fig. 1: Classification of methods for depth estimation (based on [7])

3.3.2. Active stereo vision

These systems use a stereo camera setup with an auxiliary structured light source. General approaches are evaluated in [20] and [21]. A matching method using structured light in order to improve the precision and efficiency of 3D measurement is proposed in [22]. Instead of an additional light projection a simplified stereo vision setup by using image sequences of the moving stripe lighting of a top view scanner is described in [23].

Reference [24] describes an accurate hardware-based stereo vision. A novel stereo matching algorithm to enable accurate and fast real-time stereo vision in embedded systems is proposed. A 3D measurement method based on mesh candidate and structured light for online depth recovery is described in [25].

3.3.3. Estimation of normals

Shape from texture reconstructs the 3D information about the object using the spatial distribution of surface markings [26], [27]. Shape from shading is based on a 3D geometry reconstruction from different lighting conditions using a single camera [28]. In some publications this principle is described as photometric stereo.

4. APPROACH

4.1. **Concept**

Various aspects must be considered against each other for the selection of an appropriate image processing methods for determination of geometric and surface inspection of weak textured objects. The processing speed is of crucial importance according to the requirements. The methods were compared by practical tests in order to select an appropriate method for the inspection task. Some methods could be excluded after these tests because they did not meet the above-described requirements of the inspection task. For example, scanning methods, such as laser triangulation, could be excluded because transversal movements of the object lead to inconsistent reconstruction. A comparison of the selected methods for the inspection task is shown in Fig. 2 in the form of a radar chart.

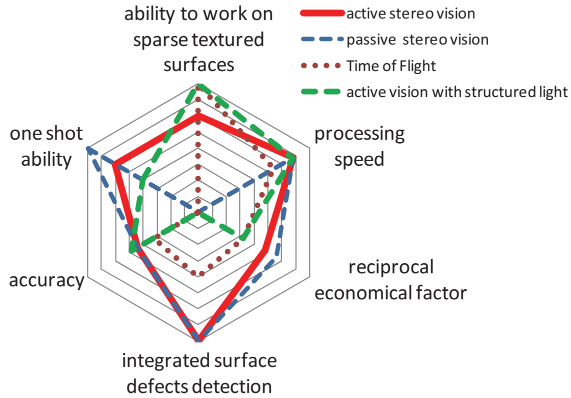

Fig. 2: Comparison of selected methods for the inspection task (based on [32])

The active stereo vision method has been selected based on comparative measurements and assessments. This method is most suitable for the task because of the short image acquisition time. Passive stereo vision shows foibles in weak or non-textured surfaces, which are due to the acquisition principle. The absence of surface texture does not allow finding a correlation of points for the stereo surface reconstruction. The passive stereo method can be improved by projecting an auxiliary pattern onto the surface, although these patterns complicate the use the obtained images for surface inspection in general. This method is appropriate here because low-textured objects are to be tested in the described application.

Alternative methods are not suitable for the stated inspection task, because a method is needed for the complete reconstruction of moving objects. In addition, the considered surfaces have no texture, which would allow finding a correlation of the points in passive stereo method. These considerations lead to a system concept based on multiple cameras grouped to active stereo modules.

4.2. **Conventional dual camera setup**

An experimental setup with a stereo module is to be implemented as a precursor for studying the basic properties and characteristics of the concept. The basic usefulness of the concept and important geometric and optical parameters to the design of the system should be investigated and determined. A conventional passive disparity stereo system consists of two rigid aligned area scan cameras. A single stereo module can accept only a partial view of three-dimensional object.

4.3. **Extended shape reconstruction with multiple stereo modules**

Several stereo modules must be used in this approach to analyze the surface and geometry of the entire 3D object with the developed system. The setup of our imaging system with two pairs of grayscale area scan cameras, laser pattern generators and customized lighting systems is illustrated in Fig. 3. Various processing steps are necessary in order to reconstruct point clouds into a common reference coordinate system.

A mesh model is generated from the point cloud in

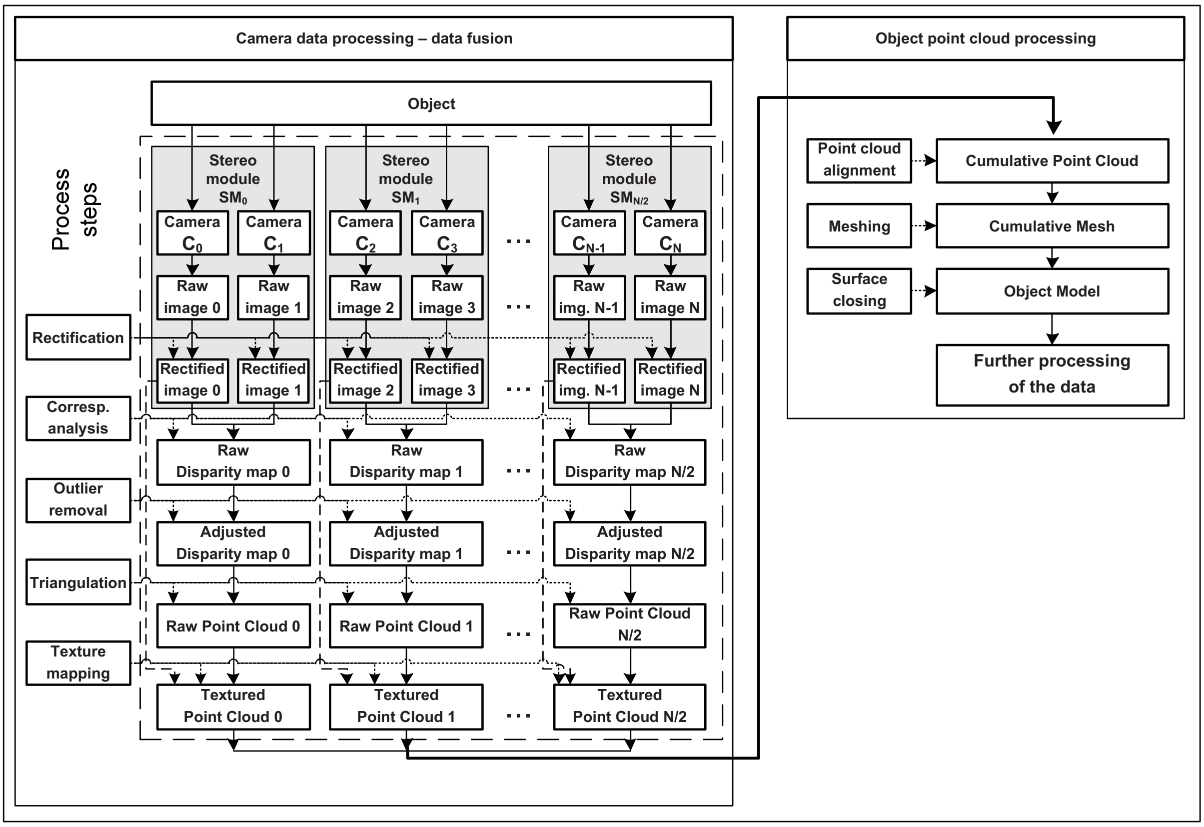

Fig. 3: Workflow for shape reconstruction from image data

the object shape from multiple views.

In the first step an image rectification is performed followed by correspondence analysis. The resulting disparity maps are filtered in order to remove the outliers. The following triangulation transforms the pixel oriented depth information in real world depth data.

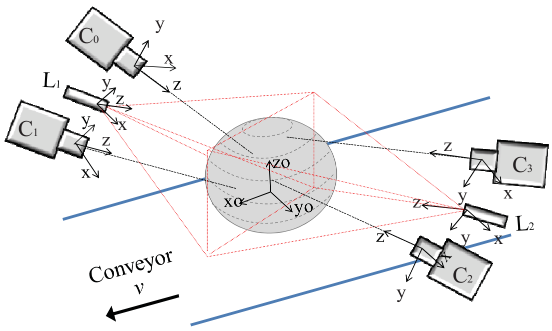

Fig. 4: Image acquisition principle concept

The intensity values from the 2D image are mapped to the generated point cloud. Thereby the texture information of the object can also be processed if the pattern structure is considered within image analysis. In the following step, the obtained point clouds are concatenated to a contiguous point cloud. This is done by transformation of all partial the subsequent meshing process. This model includes usually some areas in which there is no depth information. These areas are closed by an appropriate reconstruction method by means of data interpolation. In this case, the missing information is estimated by the present 3D information and reconstruction data based on a priori knowledge. Finally, the generated object model can be made available for further processing and applications. The whole workflow is depicted in Fig. 4.

5. EXPERIMENTS

The experiments are focused on: proof of concept, evaluation of accuracy as well as best possible parameter sets for imaging. Furthermore the setup provides us a configurable platform for field tests and further development.

The dimensions of the experimental setup are carried out according to the definition of the measurement volume as mentioned in the requirements. A system was developed consisting of two stereo modules as an example for the described multiple view system.

5.1. **Implementation**

A stereo module consists of two single monochrome area scan cameras with entocentric lenses and a laser pattern generator. The optical axes are oriented toward the part under examination and are approximately antiparallely aligned. The parallax angle and the base line of a stereo module are freely adjustable.

These values are subject of further experiments and have to be estimated with regard to the given measurement volume, geometrical configuration and optimal performance of the analyzing processing algorithms.

The lenses are selected in order to cover the measurement volume. The cameras work with ½`` CCD sensors with a resolution of 752x582 pixel, global shutter and a maximal image rate of 49 frames per second. In correlation with the sensor size, entocentric lenses have been applied with a focal length of f=8.5 mm.

In order to project a laser pattern on the surface collimated infrared laser modules with a wavelength of λ=900 nm have been used. Both a regular grid pattern and a stochastic dot pattern are generated with diffractive optical elements (DOE) and have a fan angle of approximately 40°. The laser beam provides sufficient contrast to the surface of the test objects and it can be detected well on the inspected part.

Corresponding to the requirements on feeding speed to capture the object during a movement at the same position and same time, we use a camera trigger provided by an external sensor.

5.2. **System Calibration**

In order to obtain 3D shape models with best possible quality, an accurate calibration of the single cameras, the stereo modules as well as the complete multiple view system is crucial. This is achieved in a three stage calibration procedure (Fig. 5). For single camera calibration as the first stage we apply the method described in [29].

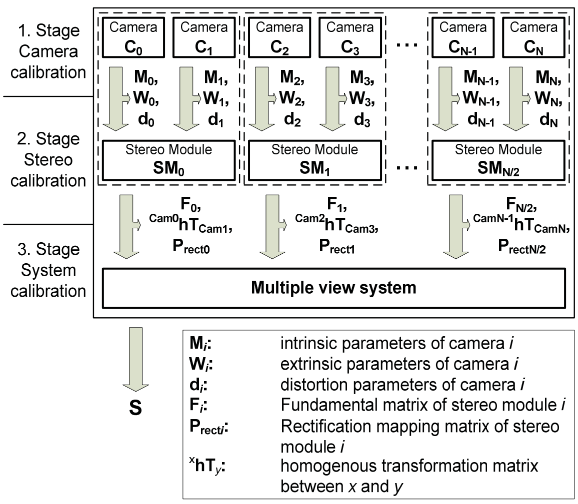

Fig. 5: Stereo modules calibration procedure workflow

The second stage is the stereo calibration according to the method of [30]. The final stage of the calibration procedure specifies the system calibration at which the spatial relations between all the stereo modules to each other have to be determined. This calibration works according to the method of absolute orientation using unit quaternions proposed by Horn [31]. The presented application is realized in the following way: Given N points in both coordinate systems of stereo module l and m, respectively the appropriate rotation R and translation t between these modules is determined by minimizing the following least squares error criterion:

$$\arg\ \min_{R,t} \sum_{i=1}^{N} \left\| P_{li} - \mathbf{R} P_{mi} - \mathbf{t} \right\|^2$$

If two stereo modules do not share the same control points, as it is the case in the presented setup, the geometrical transformation between the respective control points has to be incorporated into the computation.

According to this prerequisite a double sided calibration target with a chessboard has been used in our case. Marker points on both sides of the target are precisely aligned to each other. Generally, assuming M stereo modules, the spatial relation between these stereo modules can be described by a square matrix **S**. This matrix of dimension M x M contains the transformation matrices of all combinations:

$$\mathbf{S} = \begin{vmatrix} \mathbf{I} & {}^{SM_1}\mathbf{hT}_{SM_0} & \cdots & {}^{SM_M}\mathbf{hT}_{SM_0} \\ {}^{SM_0}\mathbf{hT}_{SM_1} & \mathbf{I} & & {}^{SM_M}\mathbf{hT}_{SM_1} \\ \vdots & \vdots & \ddots & \vdots \\ {}^{SM_0}\mathbf{hT}_{SM_M} & {}^{SM_1}\mathbf{hT}_{SM_M} & \cdots & \mathbf{I} \end{vmatrix}$$

$\mathbf{I}$: Identity matrix

In our experimental arrangement the matrix **S** has a dimension of 2 x 2 due to the number of two applied stereo modules. The whole calibration workflow is depicted in Figure 5.

5.3. **Experimental Results**

Initially the principal capability to reconstruct shapes of weak textured objects by the proposed system has been proved by our experimental setup. To get an idea of the general feasibility we used a ceramic cup as a simple representative model for weak textured parts. In numerous experiments we have evaluated important parameters, their dependencies and relevant values. It yields in relationships described in following subchapters.

5.3.1. Acquisition rate

Based on the described CCD cameras and the geometrical conditions, the developed setup allows to acquire objects with a rate of up to 6 discrete parts per second. The limiting factor here is the processing time of the stereo reconstruction algorithms. In our experiments we used a PC system with MS Windows 7/64 bit and a quad core processor Intel Core i5@ 3.7 GHz.

5.3.2. Object conveying speed

Assuming an object diameter of appr. 70 mm and an acquisition rate of 5 parts per second we are able to realize a conveying speed with a simultaneous acquisition of 0.4 m/s.

5.3.3. Parallaxe angel φ_p

A parallel orientation of the cameras (φ_p=0°) is generally optimal for a stereo arrangement. In order to improve the depth resolution in close range an inward verging between the optical axes of cameras (φ_p>0°) is recommendable. In our case considering the constrains on the given workspace (cf. requirements) an experimental value for φ_p=6° has been evaluated. Further it has been found out that a parallax angle φ_p>>0° leads to a significant drop in the number of correspondences for disparity computation

*5.3.4. Baseline of a stereo module **T***

It is generally known that a wide stereo base provides a high depth resolution. However it leads to a longer minimum working distance as well. A baseline of 90 mm results from our setup geometry.

5.3.5. Auxiliary pattern characteristic

The structure of the projected pattern is one of the most important factors for the presented approach. It largely determines the success and quality of surface reconstruction. Patterns can be basically characterized by their homogeneity and uniqueness. A homogeneous arrangement of the projected pattern as it is the case for a regular pattern leads to a steady distribution of the correlation points in the reconstructed surface model, but it increases the risk of ambiguous correlations. A high uniqueness as it is the case for a stochastic pattern reduces ambiguous assignments of correlation points, but it decreases the uniformity of the surface scan at the same time. Homogeneity and uniqueness are opposing goals, so they must be weighed against each other with care. In our previous work [32] a regular laser grid pattern with 51x51 lines has been used. Despite of generating homogenous point clouds it suffers from ambiguities especially in the case of regular shaped objects. which This might lead to fragmented point clouds and thus to a reduced number of inliers. The current improvement is to use a random dot pattern which reduces the number of ambiguities in the stereo correspondence analysis. The dots with an average diameter of 1.3 mm in the object space are randomly distributed. The pattern density ratio (cumulated dot area to covered projection area) is approximately 25%.

Within an experiment on estimating and comparing the number of inliers as well as the standard deviation due to the different pattern characteristics the RANSAC algorithm was applied to the reconstruction results of well defined geometric test targets (e.g. cube and sphere). In this special experiment, the acceptable range for the consensus of the RANSAC algorithm [33] was enlarged successively. This experiment shows in a clear distinction in performance between the grid and dot laser pattern. The number of inliers was counted and evaluated with respect to the range mentioned above. The experiments led to results described in the following.

Applying the dot pattern, the number of proper recognized surface points is significantly higher (up to factor 2.5) than using the grid pattern under the same conditions. It seems to depend on the higher uniqueness of the used dot pattern leading to a higher density of correctly reconstructed points.

The scatter of the unfiltered point cloud can be significantly improved by applying a radius based outlier removal filter. The signal to noise ratio (SNR) rises and therefore the reconstruction performance is much more reliable (Fig. 6).

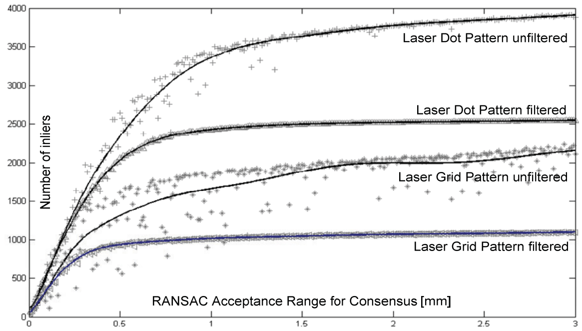

Fig. 6: Experimental results on accuracy and variation of different laser patters and filtering

5.3.6. Algorithm parameters

The images of the camera pairs are processed in a software, that was implemented in C++. Fig. 9 illustrates the general user interface of this software. The software implements the workflow as mentioned in Fig. 4. The automatic correlation of the surface points is determined by numerous parameters. Especially the parameters for adjusting the disparity range are crucial for reliable shape estimation in order to avoid ambiguities. The choice of parameters depends on the specific configuration of the camera setup and it leads to a trade-off between costs, complexity, accuracy and performance.

5.3.7. Accuracy

Experiments on accuracy of a single stereo module deliver an average depth accuracy of 0.8 mm with a standard deviation of 0.22 mm for a working distance of 200 mm. The overall accuracy of shape estimation for the given case of two opposite stereo modules results in a value of 1.2 mm with a standard deviation of 0.31 mm using a reference object “sphere” (Fig. 7) with a diameter of 120 mm.

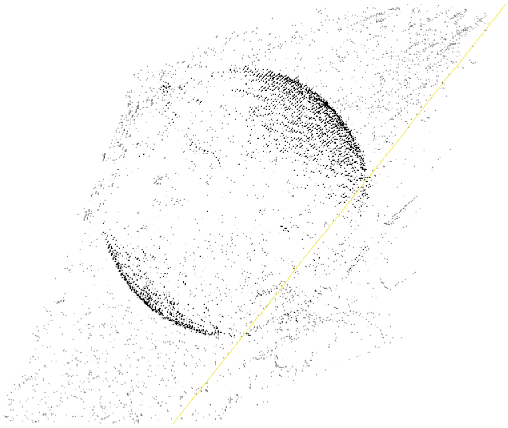

Fig. 7: Reconstruction of reference object sphere

5.3.8. Surface reconstruction performance

Tests on reconstruction performance of the experimental setup executed on the reference test object "potato tuber" reveal a significant improvement of quality in regard to a passive stereo system. Images of two exemplary test acquisitions are depicted in Fig. 8. The proposed active stereo system provided a number of approximately 3,500 valid surface points while a passive system with unstructured light delivered approximately 500 surface points in the object edges areas only. In the image acquired with the passive stereo most of the recognized surface points arise from strong edge-like structures with high grey level gradient. In the case of agricultural products there are some naturally grown artifacts. Anyhow, the active stereo approach outperforms the passive approach for the mentioned application. In contrast to the passive stereo approach the active approach always generates homogeneous point clouds.

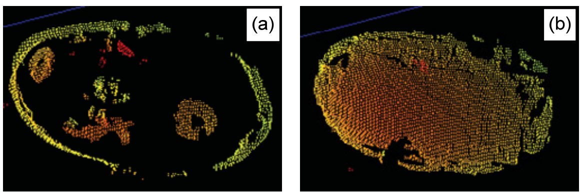

Fig. 8: Reconstruction results on weak textured surface, object potato tuber. a) acquired with passive stereo, b) acquired with active stereo with laser pattern.

6. CONCLUSION AND OUTLOOK

The aim of this paper is to present a method which is particularly suitable for 3D surface reconstruction of weak textured objects or scenes which have to be acquired by one-shot. Primarily, naturally grown agricultural products are focused in this paper. By means of the presented approach the surface and geometry of an object can be detected fast, stable and almost entirely. Weak textured surfaces can be reliably reconstructed by means of projection of auxiliary patterns. A new stochastic dot pattern has been used in order to improve the reliability of surface reconstruction. The previously used grid pattern [32] and the new dot pattern have been compared in practical experiments.

The method is suitable for the acquisition of similar in size and appearance agricultural products. If the size or appearance of the test objects varies too much, an acquisition cannot be ensured. This implies that the system has to be adapted to the desired application. The quality of the result and the processing speed of the system especially depends on an appropriate choice of the parameters for adjusting the allowed disparity search range, whereas a vague set of those parameters might lead to ambiguities, depending on the used grid pattern and inadequate processing speed. Therefore, it turns out, that a priori knowledge is always advantageous for optimum setting of algorithm parameters.

The quality of the reconstructed object model can be improved by increasing the number of stereo modules. Color cameras can be used depending on the intended application, e.g. for 3D localization of defects in an industrial inspection application. A bispectral camera (VIS/IR) can be used alternatively, in order to acquire the intensity image and the projected pattern simultaneously applying an IR laser. The method should be extended so that it can be adapted rapidly and flexibly to varying applications. In order to improve the computational speed, different computer architectures can be used; especially computations on GPUs (e.g. CUDA).

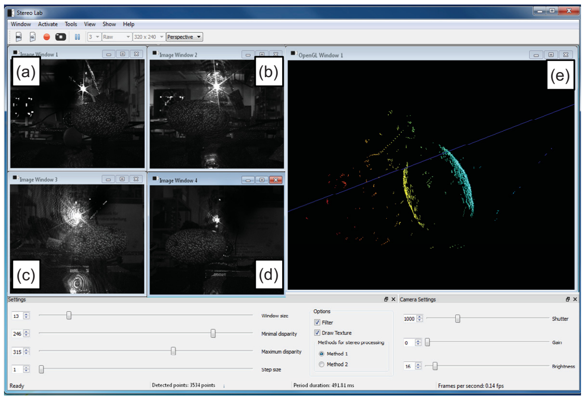

Fig. 9: GUI of developed processing software StereoLab with two camera pair views a)-d) and e) reconstructed surface of a potato tuber

7. REFERENCES

[1] M. Weyrich, P. Klein, M. Laurowski, "Optische Lokalisierung, Klassifizierung und automatische Behebung von Fehlern am Beispiel von Agrarprodukten," in *Forum Bildverarbeitung 2010*, KIT Scientific Publishing, 2010, pp. 389-400.

[2] M. Weyrich, P. Klein, M. Laurowski, Y. Wang, "Vision based Defect Detection on 3D Objects and Path Planning for Processing," in *Proceedings of 11th*

WSEAS International Conference ROCOM 2011, Venice, 2011.
[3] N. Lazaros, G. C. Sirakoulis, A. Gasteratos, “Review of Stereo Vision Algorithms: From Software to Hardware,” in *International Journal of Optomechatronics*, yr. 2, H. 4, 2008, pp. 435-462.
[4] P. Besl, “Active optical range imaging sensors,” in *Machine Vision and Applications*, Vol. 1, Springer, 1998, pp. 127–152.
[5] S. Schuon, C. Theobalt, J. Davis, S. Thrun, “High-quality scanning using time-of-flight depth superresolution,” in *IEEE Computer Society Conference on Computer Vision and Pattern Recognition Workshops*, Anchorage, Alaska 2008, pp. 1–7.
[6] M. S. Muhammad, H. Mutahira, A. Majid, T. Choi, Senior Member IEEE: “Recovering 3D Shape of Weak Textured Surfaces,” *International Conference on Computational Science and Its Application*, 2009.
[7] K. Tönnies, *Grundlagen der Bildverarbeitung*, Pearson Studium, 2005.
[8] S. Tosovic, R. Sablatnig, M. Kampel, *On Combining Shape from Silhouette and Shape from Structured Light*, Vienna University of Technology 2002, online: http://www.prip.tuwien.ac.at/~sab/../~sab/papers/cvww02.pdf, last visited: 2011-03-29.
[9] D. Scarpin; J. Wahrburg,: “Entwicklung eines robotergeführten Lichtschnittsensors für die berührungslose Erfassung anatomischer Strukturen,“ in: O. Burgert (editor), *9. Jahrestagung der Deutschen Gesellschaft für Computer- und Roboterassistierte Chirurgie e.V.*, DAV Verlag, 2010, pp. 231-235.
[10] K. Krengel-Rothensee, L. Martin-Schledde, F. Hilbk-Kortenbruck and M. Krauhausen, “Inline-Geometrieprüfung in der industriellen Fertigung,“ in *VDI-Z Integrierte Produktion*, 6-2006, Springer, Düsseldorf, 2005.
[11] F. w. DePiero and M. M. Trivedi: “3-D computer vision using structured light: Design, calibration, and implementation issues,” in *Advances in Computers*, 43, pp. 243-278, 1996.
[12] H. Kawasaki and R. Furukawa: “Dynamic scene shape reconstruction using a single structured light pattern,” in *CVPR 2008. IEEE Conference on Computer Vision and Pattern Recognition*, 2008.
[13] Online: http://www.primesense.com/, last visited: 2011-03-23.
[14] L. Song, J. Luo, B. Sun and Y. Wen, “ Two Cameras Vision Model for the 3D Shape Recovery,” in *Fifth International Conference on Natural Computation*, vol. 5, pp. 246-250, 2009.
[15] M. A. Akhloufi, “Real-time 3D visual servoing of an industrial cutting robot manipulator,” in *World Academy of Science, Engineering and Technology (WASET)* 60, 2009.
[16] Z. Ren and L. Cai, “Accurate Dimensional Measurement of 3D Round Holes Based on Stereo Vision,” in *World Academy of Science, Engineering and Technology (WASET)* 60, 2009.
[17] T. R. Arana and I. Maurtua, “ Automatic Inspection of Percussion Caps by Means of Combined 2D and 3D Machine Vision Techniques,” in *World Academy of Science, Engineering and Technology (WASET)* 64, 2010.
[18] C. Perwass, L. Wietzke, “Mikrolinsen-basierte 4D-Lichtfeldkameras zur räumlichen Bilderfassung durch ein einziges Objektiv in einer Aufnahme,“ in *Photonik,* no. 6-2010, pp. 36-40, 2010
[19] M. Amtoun, B. Boufama, “Multibaseline stereo using a single-lens camera Image Processing,” in International Conference on ICIP, vol.1, pp. I- 401-4 vol.1, 14-17, 2003.
[20] H. Hamfeld. *Aktive Stereoskopie*, Univ. Kaiserslautern, Germany, Fachbereich Informatik, 2002.
[21] D. Modrow, *Real-time active stereoscopic system for technical and biometric application*, TU Munich, Germany, 2009.
[22] G. Gao, X. Chen, H. M. Zhang, “A Fast Structured Light Matching Method in Robot Stereo Vision,” in *Journal Applied Mechanics and Materials*, vol. 29 - 32, pp. 1981-1984, 2010.
[23] E. Lilineblum, R. Niese and B. Michaelis, “A Stereo Vision System for Top View Book Scanners,” *World Academy of Science, Engineering and Technology (WASET)* 59, 2009.
[24] K. Ambrosch, W. Kubinger, “Accurate hardware-based stereo vision,” in *Journal of Computer Vision and Image Understanding*, vol. 114, issue 11, Elsevier Science, New York, NY, 2010.
[25] G. Xu and B. Liu, “A Mesh-candidate-based 3D Reconstruction System for Online Depth Recovery,” in *2nd International Conference on Computer Engineering and Technology*, Int J Comput, vis 84, pp. 257-268, 2009.
[26] B. J. Super, A. C. Bovik, “Shape from texture using local spectral Moments,” *IEEE Transactions on Pattern Analysis and Machine Intelligence*, vol. 17, no. 4, pp. 333-343, 1995.
[27] A. P. Witkin, “Recovering surface shape and orientation from texture,” *Artificial Intelligence*, vol. 17, pp. 17-45, 1981.
[28] Z. Zhang, “A flexible new technique for camera calibration,” *IEEE Transactions on Pattern Analysis and Machine Intelligence 22*, 1330-1334, 2000.
[29] R. Zhang, P.-S. Tsai, J. E. Cryer, M. Shah, “Shape from Shading: A Survey, “ in *IEEE Transactions on Pattern Analysis and Machine Intelligence*, year 21, pp. 690-706, 1999.
[30] J.-Y. Bouget *Camera calibration toolbox for Matlab*, online: http://www.vision.caltech.edu/bouguetj/calib_doc/htmls/example5.htm, last visited: 2011-03-29.
[31] B. K. P. Horn, “Closed-form solution of absolute orientation using unit quaternions,” in *Journal of the Optical Society of America*, pp. 4:629–642, 1987.

[32] Thomas Kerstein, Martin Laurowski, Philipp Klein, Michael Weyrich, Hubert Roth, Jürgen Wahrburg, *Optical 3D-Surface Reconstruction of Weak Textured Objects Based on an Approach of Disparity Stereo Inspection.*, In: Proceedings of International Conference on Pattern Recognition and Computer Vision (ICPRCV 2011), issue 78, p. 581-586, Amsterdam, Netherlands , 2011

[33] Martin A. Fischler und Robert C. Bolles: Random Sample Consensus: *A Paradigm for Model Fitting with Applications to Image Analysis and Automated Cartography*. Communications of the ACM, Volume 24, Number 6, June 1981.